Light-Activatable TET-Dioxygenases Reveal Dynamics of 5-Methylcytosine Oxidation and Transcriptome Reorganization

Shubhendu Palei, Benjamin Buchmuller, Jan Wolffgramm, Álvaro Muñoz-Lopez, Sascha Jung, Paul Czodrowski and Daniel Summerer*

Faculty of Chemistry and Chemical Biology, TU Dortmund University, Otto-Hahn-Str. 6, 44227 Dortmund (Germany)

ABSTRACT: Ten-eleven-translocation (TET) dioxygenases catalyze the oxidation of 5-methylcytosine (5mC), the central epigenetic regulator of mammalian DNA. This activity dynamically reshapes epigenome and transcriptome by depositing oxidized 5mC derivatives, and initiating active DNA demethylation. However, studying this dynamic is hampered by the inability to selectively activate individual TETs with temporal control in cells. We report activation of TETs in mammalian cells by incorporation of genetically encoded 4,5-dimethoxy-2-nitrobenzyl-L-serine as transient active site block, and its subsequent deprotection with light. Our approach enables precise insights into the impact of cancer-associated TET2 mutations on the kinetics of TET2 catalysis *in vivo*, and allows time-resolved monitoring of target gene activation and transcriptome reorganization. This sets a basis for dissecting the order and kinetics of chromatin-associated events triggered by TET catalysis, ranging from DNA demethylation to chromatin and transcription regulation.

5-Methylcytosine (5mC, (Scheme 1) is a dynamic regulatory element of mammalian genomes with important roles in differentiation, development and carcinogenesis.[1-2] In mammals, the three ten-eleven translocation dioxygenases TET1, TET2, and TET3 catalyze the iterative oxidation of 5mC to 5-hydroxymethyl-, 5-formyl, and 5-carboxylcytosine (5hmC, 5fC and 5caC, Scheme 1) in an iron-, oxygen- and α-ketoglutarate-(αKG)-dependent fashion. These nucleobases are intermediates of active DNA demethylation,[3-4] but also possess inherent regulatory functions via specific interactions with key nuclear proteins,[5-8] and influence on nucleosome stability[9] and positioning.[10]

Studying how normal and aberrant TET catalysis dynamically reorganizes epigenome and transcriptome is key to understand the emergence of cellular phenotypes during (de-) differentiation and malignant transformation. For example, TET2 is mutated in a wide range of cancers. This can perturb 5mC oxidation and target gene activation by directly affecting the general catalytic activity or nucleobase preference,[11] or by altering protein- and target gene interactions.[12] However, studying in-cell kinetics of 5mC oxidation and its downstream events by individual TETs or TET mutants requires their selective activation at defined time points. This would overcome system noise and enable uncoupling the kinetics of catalysis itself from potentially rate-limiting upstream processes in the TET life cycle.

Compared to general approaches to control protein expression (such as Tet on/off systems or siRNA knock-downs[13]), small molecule TET effectors provide direct control with enhanced temporal resolution, but are restricted to mere inhibition of constitutively active TETs. Moreover, the existence of >60 homologous, αKG-dependent dioxygenases in human represents a severe selectivity challenge[14] (a recent bump-and-hole strategy provides a new impulse to circumvent this problem[15]). In contrast, optochemical strategies provide unparalleled spatiotemporal control by employing photoresponsive substrates and proteins.[16-17] Here, the genetic encoding[18-20] of photocaged noncanonical amino acids (ncAA) allows for precise control of protein functions by expression in an inactive state, and activation with light.[21] This strategy is highly modular, allows selective control of individual protein homologues, and can be applied with spatial resolution, i.e. by irradiating parts of cells, cell populations, or organisms.[22-31]

Scheme 1: Light-activated oxidation of 5mC by photocaged TET and downstream events.

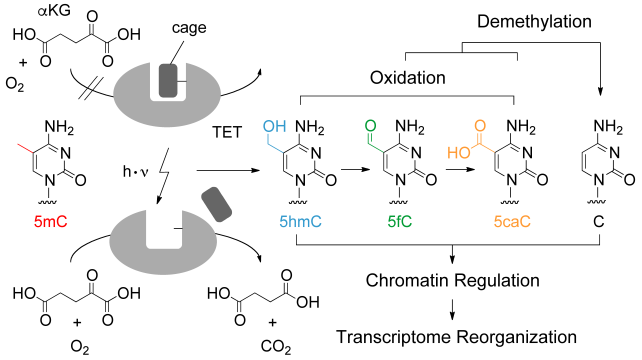

We aimed at developing photoactivatable TETs by replacing active site residues with a photocaged ncAA. The caging group may thereby inhibit catalysis or cofactor binding, and active TET could be generated *in situ* by light irradiation (Scheme 1). We chose the ncAA 4,5-dimethoxy-2-nitrobenzyl-L-serine **1** (Fig. 1a) that can be genetically encoded by an *Escherichia coli* amber suppressor leucyl-tRNA-synthetase (LRS)/tRNA^{Leu} pair.[22-23] Using the murine TET2 catalytic domain as model (Fig. 1b, hereafter "mTET2"), we evaluated three active site serines/threonines for substitution, based on crystal structures and mutational studies.[11, 32] At S1203, modeling suggested that the presence of **1** affects the orientation of the 5mC nucleobase, albeit with unaltered positions of the 5-methyl group, the iron ion and the αKG analog N-oxalylglycine NOG (Fig. 1c). At T1285, the caging group leads to repositioning of 5mC, NOG and iron, the latter involving coordination by the 5mC N4-amino group. However, at S1812, **1** completely displaces NOG, and strongly repositions iron and 5mC (Fig. 1c).

We constructed vectors encoding mTET2 with C-terminal HA-tag and without (wild type, wt) or with a single amber codon at each of the candidate positions (Fig. 1b). We co-transfected each vector with pLRS_BH5 (encoding LRS/tRNA^{Leu}) in HEK293T cells, which exhibit a low background of oxidized 5mCs[33] for later kinetic studies with high dynamic range. After expression for 24 h in presence or absence of 0.1 mM **1**, we fixed and permeabilized the cells, and analyzed the expression of full-length protein by anti-HA immunostainings and flow cytometry (FCM).

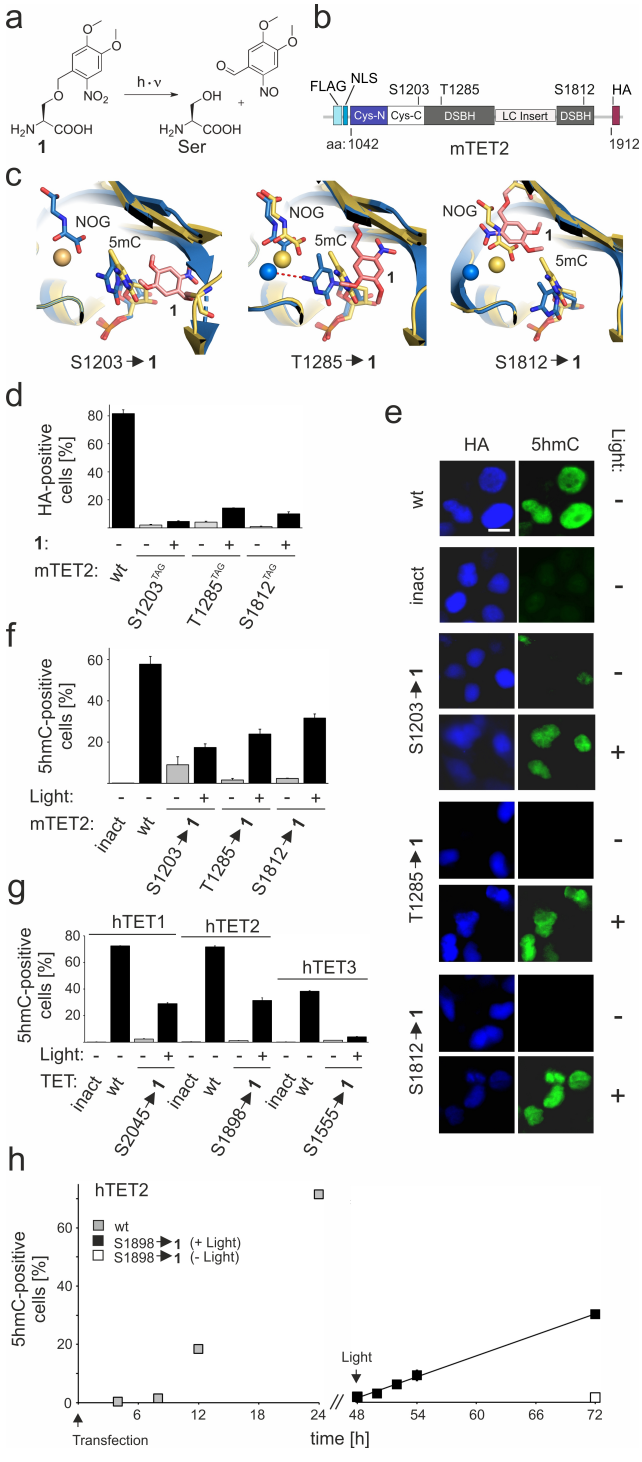

Figure 1: Light-activated 5mC oxidation by TET in HEK293T cells. a) Decaging of photocaged serine **1**. b) Features of mTET2 catalytic domain construct and amber positions for incorporation of **1**. c) Models of mTET2_S1203→**1**, T1285→**1** and S1812→**1** active sites (blue), superimposed with crystal structure of hTET2_wt (yellow, pdb 4NM6[32]). **1** is shown in rose, iron as spheres. d) Incorporation of **1** at mTET2 amber codons analyzed by anti-HA immunostaining and FCM. e) Anti-HA and anti-5hmC co-immunostainings of cells expressing indicated mTET2 constructs with or without light irradiation. Scale bar: 10 µm. f) Anti-5hmC immunostainings and FCM analysis of cells expressing the indicated mTET2 constructs, 24 h after light or no light. g) As Fig. 1f for hTET1, 2 and 3. h) Kinetics of 5hmC formation for constitutively active wt hTET2, and for caged hTET2_S1898→**1** quantified by FCM. Line from linear regression.

We observed varying mTET2 expression levels in the cell populations for mTET2_S1203^{TAG}, _T1285^{TAG} and _S1812^{TAG} vectors in presence of **1**. These were strongly reduced in its absence, indicating incorporation of **1** with high fidelity (Fig. 1d; additional fidelity control in SI Fig. 2).

We next asked, if our approach enables translation of mTET2 in fully inactive form, and if light irradiation leads to activation and global oxidation of 5mC to 5hmC. After expression for 24 h, we removed **1** from cultures to stop mTET2 expression, and irradiated them with light (3 min, 365 nm) or not. After additional 24 h, we imaged the cells after anti-HA and anti-5hmC co-immunostainings. Cultures expressing wt mTET2 or a catalytically inactive mutant (H1295Y/D1297A, first described for mTET1[34]) showed high 5hmC signals only for the former (Fig. 1e and SI Fig. 4). Moreover, all mTET2 amber mutants showed high 5hmC formation only after light activation, indicating successful decaging. mTET2_S1203→**1** thereby exhibited a weak 5hmC signal without light, indicating incomplete inactivation (Fig. 1e). This is in agreement with the model that suggests no influence of **1** on the positions of NOG, iron and the 5-methyl-group (Fig. 1c). Quantification of 5hmC by FCM confirmed this residual activity of mTET2_S1203→**1**, but also revealed for mTET2_S1285→**1** and _S1812→**1** high 5hmC formation (41 % and 55 % compared to wt) and minimal background (Fig. 1f and SI Fig. 5; see SI for analyses by mean 5hmC signal of HA-positive cells). We proceeded with mTET2_S1812→**1**, because of its high activation (tunable by light-dosage, see SI Fig. 7), and the ability to generate wt mTET2 without T→S mutation.

We next tested, if this caging strategy would be broadly applicable also to human TETs. We expressed the human TET1, 2 and 3 catalytic domains (hereafter "hTETs") with incorporation of **1** at positions corresponding to mTET2_S1812. FCM analysis of HA/5hmC showed light-activation and minimal background in all three cases, though hTET3 exhibited a comparably low intrinsic activity (Fig. 1g and SI).

Current studies of TET catalysis are restricted either to *in vitro* measurements or to the expression of constitutively active TETs. This prevents studying TET *in vivo* kinetics independently from kinetics of upstream processes, such as expression, folding and posttranslational modification. Indeed, non-caged wt hTET2 exhibits complex kinetics with a lagged, nonlinear 5hmC increase after transfection (Fig. 1h). In contrast, light-activation of hTET2 S1898→**1** 48 h after transfection and at a constant, saturated expression level shows strict linear kinetics (Fig. 1h and SI Fig. 12).

With these tools in hand, we aimed to study the impact of cancer-associated TET2 mutations on *in vivo* catalysis. TET2 is

one of the most frequently mutated genes in hematopoietic malignancies,[12] with >35% of mutations being missense mutations with poorly understood roles, many scattered over the catalytic domain.[35] This globular domain comprises two Cys-rich subdomains (CysN/C) and a double-stranded β helix (DSBH) domain with a low-complexity (LC) insert (Fig. 2a).[32] We selected a panel of frequent catalytic domain mutations (Fig. 2a-b and SI Table 4), some with previous characterization by traditional approaches. Activation and FCM analysis of cells with the same HA levels 24 h later revealed a broad range of 5hmC levels (Fig. 2c and SI).

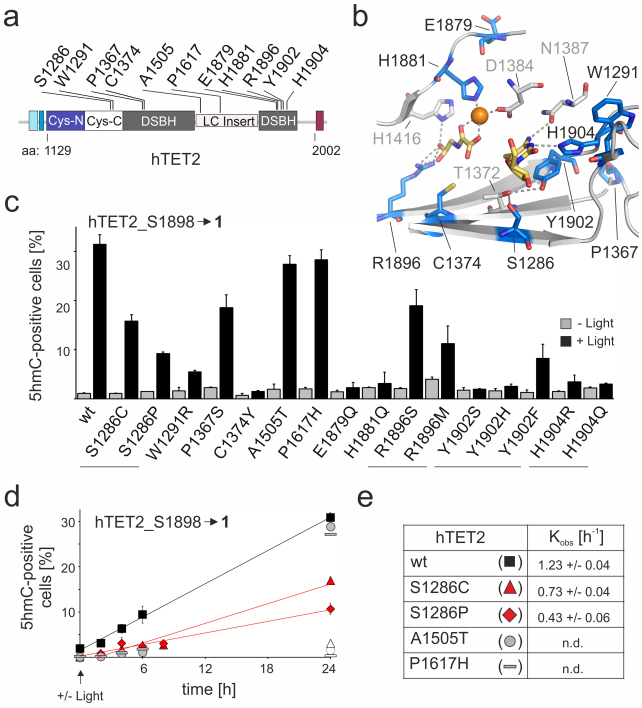

Figure 2: Light-activation and in-cell kinetic studies of cancer-associated hTET2 mutants. a) Features of hTET2 catalytic domain with cancer-associated mutant positions. b) Crystal structure of hTET2_wt active site (4NM6[32]). Analyzed positions shown in blue, 5mC and NOG in yellow. c) Analysis of 5hmC formation by hTET2 mutants. d) Kinetics of 5hmC formation for selected hTET2 mutants. K_{obs} obtained by linear regression. Unfilled marker: control without light.

Mutations of H1881 and H1904 that directly interact with iron or 5mC completely abolished activity (Fig. 2b-c). This is in agreement with traditional analyses, and shows that these mutations directly affect TET catalysis also *in vivo*.[36] Interestingly, deactivation was also observed for the two uncharacterized mutations Y1902S/H. Y1902 is stacking against the 5mC pyrimidine, and an exchange to A abolishes activity,[36] whereas F can partially rescue this function[11] (Fig. 2c). Our finding indicates that the aromatic H is not able to play a similar role. Next, the known mutations W1291R, P1367, E1879Q with potential structural impact, and mutations R1896S/M likely affecting αKG coordination showed varying activity losses, similar to ones reported for constitutively active TET2 mutants (Fig. 2c).[36-37] Particularly interesting were the uncharacterized mutations C1374Y and S1286C/P (at the active site bottom, Fig. 2b). C1374Y abolished activity, which may be explained by steric interference with αKG-binding. Instead, both mutations of S1286 showed only a slight reduction in activity (Fig. 2c). This residue builds a hydrogen bond network with T1372 and the 5mC-stacking Y1902.[11] For precise quantification, we performed time-resolved experiments and calculated observable rate constants (K_{obs}, Fig. 2d). The nonpolar, isosteric S1286C mutation and the nonpolar, structurally deviating S1286P mutation led to 1.7-fold and 2.9-fold reduced activity, respectively. This supports the stabilizing function of S1286 in respect to T1372/Y1902, but also indicates a sensitivity of this position to structural perturbation, independently of this function. Finally, we analyzed A1505T and P1617H, both located in the LC insert. Both residues show markedly decreased activity *in vitro* and when expressed in constitutively active form in HEK293T cells.[38] Surprisingly, we observed virtually unaltered 5hmC levels for both mutants compared to wt hTET2 after 24 h (Fig. 2c). However, time-resolved analysis revealed slow initial rates with a rate-enhancement over time (Fig. 2d). This has not been observed in previous analyses and could hint at an additional layer of regulation, such as a positive feedback via TET-induced upregulation of factors that facilitate target recruitment or stimulate catalytic activity of TET.

5hmC is enriched at active chromatin such as enhancers and promoters, and TETs are involved in transcription regulation either independently of their catalytic function, or by deposition of oxidized 5mCs and potential subsequent demethylation.[3-4] We aimed at monitoring the kinetics of transcription activation triggered by hTET2 catalysis itself. We measured mRNA levels of the TET2 target gene ARC[39] after light-activation of hTET2 S1898→**1** (Fig. 3a). Activation indeed triggered mRNA upregulation by 3.5-fold after 24 h, with a linear behavior (Fig. 3a-b).

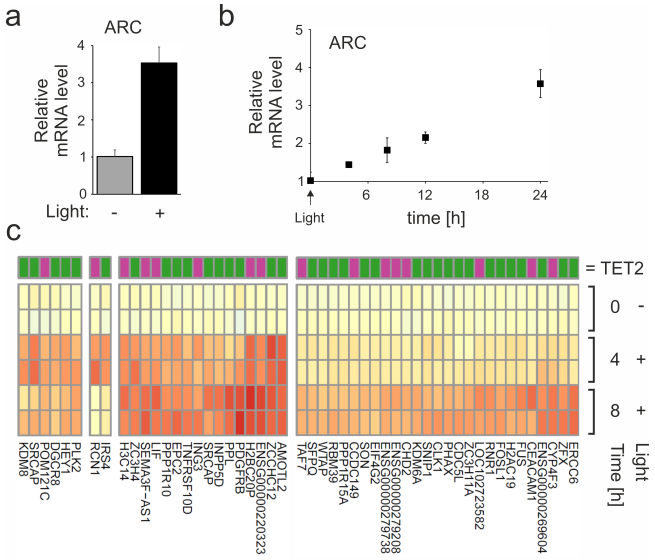

Figure 3: Light-activated target gene activation and transcriptome reorganization by hTET2 in HEK293T cells. a) mRNA upregulation of ARC by hTET2_S1898→**1**. Data from RT-qPCR normalized to GAPDH housekeeping gene control. b) Time-resolved induction of ARC. c) Gene expression patterns from mRNA-seq 4h and 8h after light-activation of hTET2_S1898→**1**. Above: presence (green) or absence (magenta) of TET2 ChIP peaks in Ref[39]. Two groups of differentially expressed genes with distinct expression patterns (duplicates, full image in SI Fig. 18) at a log2-fold change >0.26 (20%) with respect to 0 h and an adjusted p-value of <0.001.

Finally, we studied early events following hTET2 activation on a system-wide level by mRNA-seq 4h and 8h after light. In accordance with a previous study in HEK293T, we did not observe upregulation of genes involved in active demethyla-

tion[13] (full data in SI Fig. 15-18 and SI Tables 5-13). However, a large number of genes showing upregulation had known or suspected roles in transcription regulation (e.g. FUS, CDCL5, ING3, ZC3H4, HEY1), RNA processing (e.g. CLK1, SFPQ, DGCR8), N6-adenosine methylation (WTAP) or chromatin regulation (e.g. H2AC19, H3C14, CHD2, SRCAP, KDMs, Fig. 3c and SI Fig. 18). Interestingly, 65 % of the genes we found to be differentially regulated also showed TET2 signals in or near their promoters in a previous TET2 ChIP-Seq analysis (Fig. 4c and SI).[39]

In conclusion, we report light-activation of individual TET dioxygenases *in vivo*. Our strategy proves highly robust, with successful application to diverse TETs and TET mutants. Light activation enables kinetic studies of TET catalysis *in vivo*, delivering insights into the functional impact of frequent cancer mutations. We further demonstrate time-resolved monitoring of target gene activation and transcriptome reorganization, and observe how TET2 dynamically regulates genes involved in chromatin regulation as well as mRNA transcription and processing. This sets a basis for dissecting the order and kinetics of a broad range of chromatin-associated events triggered by TET catalysis on the global and local level.

ASSOCIATED CONTENT

Supporting Information. DNA/protein sequences and biochemical data. This material is available free of charge via the Internet at http://pubs.acs.org."

AUTHOR INFORMATION

Corresponding Author

*daniel.summerer@tu-dortmund.de

Funding Sources

No competing financial interests. This work was supported by the ERC (Grant EPICODE).

ACKNOWLEDGMENT

We thank P. G. Schultz for plasmid pescLRS_NVOC_BH5-4. We thank A. Rao for plasmids FH-TET1-pEF and FH-TET3-pEF, C. Gersbach for plasmid pcDNA3.1-GoldenGate-VP64, and Y. Zhang for plasmid pcDNA3-Tet2 obtained via Addgene. Structures in Fig. 2 and 3 have been prepared with PyMOL, Version 2.3.0 Schrödinger, LLC. We thank Jochen Imig and co-workers for helpful discussions.

REFERENCES

1. Bird, A., DNA methylation patterns and epigenetic memory. *Genes. Dev*. **2002,** *16* (1), 6-21.
2. Smith, Z. D.; Meissner, A., DNA methylation: roles in mammalian development. *Nat. Rev. Genet*. **2013,** *14* (3), 204-220.
3. Wu, X. J.; Zhang, Y., TET-mediated active DNA demethylation: mechanism, function and beyond. *Nat. Rev. Genet*. **2017,** *18* (9), 517-534.
4. Carell, T.; Kurz, M. Q.; Muller, M.; Rossa, M.; Spada, F., Non-canonical Bases in the Genome: The Regulatory Information Layer in DNA. *Angew. Chem. Int. Ed. Engl*. **2018,** *57* (16), 4296-4312.
5. Spruijt, C. G.; Gnerlich, F.; Smits, A. H.; Pfaffeneder, T.; Jansen, P. W.; Bauer, C.; Munzel, M.; Wagner, M.; Muller, M.; Khan, F.; Eberl, H. C.; Mensinga, A.; Brinkman, A. B.; Lephikov, K.; Muller, U.; Walter, J.; Boelens, R.; van Ingen, H.; Leonhardt, H.; Carell, T.; Vermeulen, M., Dynamic readers for 5-(hydroxy)methylcytosine and its oxidized derivatives. *Cell* **2013,** *152* (5), 1146-1159.
6. Du, Q.; Luu, P. L.; Stirzaker, C.; Clark, S. J., Methyl-CpG-binding domain proteins: readers of the epigenome. *Epigenomics* **2015,** *7* (6), 1051-1073.
7. Hashimoto, H.; Olanrewaju, Y. O.; Zheng, Y.; Wilson, G. G.; Zhang, X.; Cheng, X. D., Wilms tumor protein recognizes 5-carboxylcytosine within a specific DNA sequence. *Genes Dev*. **2014,** *28* (20), 2304-2313.
8. Kellinger, M. W.; Song, C. X.; Chong, J.; Lu, X. Y.; He, C.; Wang, D., 5-formylcytosine and 5-carboxylcytosine reduce the rate and substrate specificity of RNA polymerase II transcription. *Nat. Struct. Mol. Biol*. **2012,** *19* (8), 831-833.
9. Ngo, T. T.; Yoo, J.; Dai, Q.; Zhang, Q.; He, C.; Aksimentiev, A.; Ha, T., Effects of cytosine modifications on DNA flexibility and nucleosome mechanical stability. *Nat. Commun*. **2016,** *7*, 10813.
10. Raiber, E. A.; Portella, G.; Cuesta, S. M.; Hardisty, R.; Murat, P.; Li, Z.; Iurlaro, M.; Dean, W.; Spindel, J.; Beraldi, D.; Liu, Z.; Dawson, M. A.; Reik, W.; Balasubramanian, S., 5-Formylcytosine organizes nucleosomes and forms Schiff base interactions with histones in mouse embryonic stem cells. *Nat. Chem*. **2018,** *10* (12), 1258-1266.
11. Liu, M. Y.; Torabifard, H.; Crawford, D. J.; DeNizio, J. E.; Cao, X. J.; Garcia, B. A.; Cisneros, G. A.; Kohli, R. M., Mutations along a TET2 active site scaffold stall oxidation at 5-hydroxymethylcytosine. *Nat. Chem. Biol*. **2017,** *13* (2), 181-187.
12. Rasmussen, K. D.; Helin, K., Role of TET enzymes in DNA methylation, development, and cancer. *Genes Dev*. **2016,** *30* (7), 733-750.
13. Jin, C.; Qin, T.; Barton, M. C.; Jelinek, J.; Issa, J. P., Minimal role of base excision repair in TET-induced global DNA demethylation in HEK293T cells. *Epigenetics* **2015,** *10* (11), 1006-1013.
14. Loenarz, C.; Schofield, C. J., Expanding chemical biology of 2-oxoglutarate oxygenases. *Nat. Chem. Biol*. **2008,** *4* (3), 152-156.
15. Sudhamalla, B.; Wang, S.; Snyder, V.; Kavoosi, S.; Arora, S.; Islam, K., Complementary Steric Engineering at the Protein-Ligand Interface for Analogue-Sensitive TET Oxygenases. *J. Am. Chem. Soc*. **2018,** *140* (32), 10263-10269.
16. Ankenbruck, N.; Courtney, T.; Naro, Y.; Deiters, A., Optochemical Control of Biological Processes in Cells and Animals. *Angew. Chem. Int. Ed. Engl*. **2018,** *57* (11), 2768-2798.
17. Brieke, C.; Rohrbach, F.; Gottschalk, A.; Mayer, G.; Heckel, A., Light-controlled tools. *Angew. Chem. Int. Ed. Engl*. **2012,** *51* (34), 8446-8476.
18. Xiao, H.; Schultz, P. G., At the Interface of Chemical and Biological Synthesis: An Expanded Genetic Code. *CSH Persp. Biol*. **2016,** *8* (9).
19. Chin, J. W., Expanding and reprogramming the genetic code. *Nature* **2017,** *550* (7674), 53-60.
20. Wang, L., Engineering the Genetic Code in Cells and Animals: Biological Considerations and Impacts. *Acc. Chem. Res*. **2017,** *50* (11), 2767-2775.
21. Courtney, T.; Deiters, A., Recent advances in the optical control of protein function through genetic code expansion. *Curr. Opin. Chem. Biol*. **2018,** *46*, 99-107.,
22. Lemke, E. A.; Summerer, D.; Geierstanger, B. H.; Brittain, S. M.; Schultz, P. G., Control of protein phosphorylation with a genetically encoded photocaged amino acid. *Nat. Chem. Biol*. **2007,** *3* (12), 769-772.
23. Kang, J. Y.; Kawaguchi, D.; Coin, I.; Xiang, Z.; O'Leary, D. D. M.; Slesinger, P. A.; Wang, L., In Vivo Expression of a Light-Activatable Potassium Channel Using Unnatural Amino Acids. *Neuron* **2013,** *80* (2), 358-370.
24. Gautier, A.; Deiters, A.; Chin, J. W., Light-activated kinases enable temporal dissection of signaling networks in living cells. *J. Am. Chem. Soc*. **2011,** *133* (7), 2124-2127.
25. Nguyen, D. P.; Mahesh, M.; Elsasser, S. J.; Hancock, S. M.; Uttamapinant, C.; Chin, J. W., Genetic Encoding of Photocaged Cysteine Allows Photoactivation of TEV Protease in Live Mammalian Cells. *J. Am. Chem. Soc*. **2014,** *136* (6), 2240-2243.
26. Walker, O. S.; Elsasser, S. J.; Mahesh, M.; Bachman, M.; Balasubramanian, S.; Chin, J. W., Photoactivation of Mutant Isocitrate Dehydrogenase 2 Reveals Rapid Cancer-Associated Metabolic and Epigenetic Changes. *J. Am. Chem. Soc*. **2016,** *138* (3), 718-721.
27. Gautier, A.; Nguyen, D. P.; Lusic, H.; An, W. A.; Deiters, A.; Chin, J. W., Genetically Encoded Photocontrol of Protein Localization in Mammalian Cells. *J. Am. Chem. Soc*. **2010,** *132* (12), 4086.
28. Ren, W.; Ji, A.; Ai, H. W., Light Activation of Protein Splicing with a Photocaged Fast Intein. *J. Am. Chem. Soc*. **2015,** *137* (6), 2155-2158.
29. Bocker, J. K.; Friedel, K.; Matern, J. C. J.; Bachmann, A. L.; Mootz, H. D., Generation of a Genetically Encoded, Photoactivatable Intein for the Controlled Production of Cyclic Peptides. *Angew. Chem. Int. Ed. Engl*. **2015,** *54* (7), 2116-2120.
30. Arbely, E.; Torres-Kolbus, J.; Deiters, A.; Chin, J. W., Photocontrol of tyrosine phosphorylation in mammalian cells via genetic encoding of photocaged tyrosine. *J. Am. Chem. Soc*. **2012,** *134* (29), 11912-11915.

31. Wang, J.; Liu, Y.; Liu, Y.; Zheng, S.; Wang, X.; Zhao, J.; Yang, F.; Zhang, G.; Wang, C.; Chen, P. R., Time-resolved protein activation by proximal decaging in living systems. *Nature* **2019,** *569* (7757), 509-513.
32. Hu, L.; Li, Z.; Cheng, J.; Rao, Q.; Gong, W.; Liu, M.; Shi, Y. G.; Zhu, J.; Wang, P.; Xu, Y., Crystal structure of TET2-DNA complex: insight into TET-mediated 5mC oxidation. *Cell* **2013,** *155* (7), 1545-1555.
33. Liu, S.; Wang, J.; Su, Y.; Guerrero, C.; Zeng, Y.; Mitra, D.; Brooks, P. J.; Fisher, D. E.; Song, H.; Wang, Y., Quantitative assessment of Tet-induced oxidation products of 5-methylcytosine in cellular and tissue DNA. *Nucleic Acids Res*. **2013,** *41* (13), 6421-6429.
34. Tahiliani, M.; Koh, K. P.; Shen, Y.; Pastor, W. A.; Bandukwala, H.; Brudno, Y.; Agarwal, S.; Iyer, L. M.; Liu, D. R.; Aravind, L.; Rao, A., Conversion of 5-methylcytosine to 5-hydroxymethylcytosine in mammalian DNA by MLL partner TET1. *Science* **2009,** *324* (5929), 930-935.
35. Forbes, S. A.; Beare, D.; Gunasekaran, P.; Leung, K.; Bindal, N.; Boutselakis, H.; Ding, M.; Bamford, S.; Cole, C.; Ward, S.; Kok, C. Y.; Jia, M.; De, T.; Teague, J. W.; Stratton, M. R.; McDermott, U.; Campbell, P. J., COSMIC: exploring the world's knowledge of somatic mutations in human cancer. *Nucleic Acids Res*. **2015,** *43* (Database issue), D805-811.
36. Ko, M.; Huang, Y.; Jankowska, A. M.; Pape, U. J.; Tahiliani, M.; Bandukwala, H. S.; An, J.; Lamperti, E. D.; Koh, K. P.; Ganetzky, R.; Liu, X. S.; Aravind, L.; Agarwal, S.; Maciejewski, J. P.; Rao, A., Impaired hydroxylation of 5-methylcytosine in myeloid cancers with mutant TET2. *Nature* **2010,** *468* (7325), 839-843.
37. Fraietta, J. A.; Nobles, C. L.; Sammons, M. A.; Lundh, S.; Carty, S. A.; Reich, T. J.; Cogdill, A. P.; Morrissette, J. J. D.; DeNizio, J. E.; Reddy, S.; Hwang, Y.; Gohil, M.; Kulikovskaya, I.; Nazimuddin, F.; Gupta, M.; Chen, F.; Everett, J. K.; Alexander, K. A.; Lin-Shiao, E.; Gee, M. H.; Liu, X. J.; Young, R. M.; Ambrose, D.; Wang, Y.; Xu, J.; Jordan, M. S.; Marcucci, K. T.; Levine, B. L.; Garcia, K. C.; Zhao, Y. B.; Kalos, M.; Porter, D. L.; Kohli, R. M.; Lacey, S. F.; Berger, S. L.; Bushman, F. D.; June, C. H.; Melenhorst, J. J., Disruption of TET2 promotes the therapeutic efficacy of CD19-targeted T cells. *Nature* **2018,** *558* (7709), 307-312.
38. Wang, Y.; Xiao, M.; Chen, X.; Chen, L.; Xu, Y.; Lv, L.; Wang, P.; Yang, H.; Ma, S.; Lin, H.; Jiao, B.; Ren, R.; Ye, D.; Guan, K. L.; Xiong, Y., WT1 recruits TET2 to regulate its target gene expression and suppress leukemia cell proliferation. *Mol. Cell.* **2015,** *57* (4), 662-673.
39. Peng, L.; Li, Y.; Xi, Y.; Li, W.; Li, J.; Lv, R.; Zhang, L.; Zou, Q.; Dong, S.; Luo, H.; Wu, F.; Yu, W., MBD3L2 promotes Tet2 enzymatic activity for mediating 5-methylcytosine oxidation. *J. Cell. Sci.* **2016,** *129* (5), 1059-1071.

Table of Contents Artwork